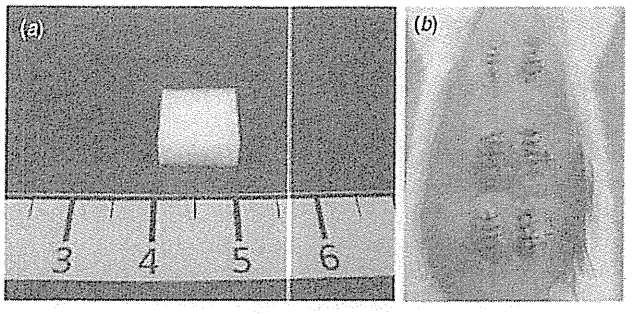

Figure 3. Collagen fiber scaffold and appearance just after it is embedded under the skin, (*a*) collagen fiber scaffold 1 cm × 1 cm × 5 mm, (*b*) appearance just after embedding the collagen fiber scaffold under the back skin of a rat.

3–0 nylon sutures (figure 3(*b*)). Tissue evaluation was performed 2 weeks after the procedure.

In order to evaluate the effect of collagen fiber orientation in the scaffold, three samples with orientation, and 3 samples without orientation were used. In the preliminary study, we found that scaffolds processed at 140 °C for 24 h had poor biocompatibility; therefore, we used these conditions in order to evaluate only the effect of collagen fiber orientation. Tissue evaluation was performed 1 week after the operation, since it is ideal for cellular infiltration of the scaffold to occur in the early stage of implantation.

All surgical experiments were performed according to the Principle of Laboratory Animal Care advocated by the Animal Research Committee of Kyoto University (2007).

2.3. Evaluation

2.3.1. Histology. Two weeks after scaffold implantation, the rats were killed by an overdose injection (intraperitoneal) of sodium pentobarbital. The back skin of each rat was stripped and fixed with 4% paraformaldehyde for more than 72 h at room temperature. All samples were extracted with skin, then dehydrated through ascending alcohol concentrations, embedded in paraffin, serially sectioned (4 μm) in the perpendicular plane, dewaxed and stained with hematoxylin-eosin (H–E). Thereafter, the sections were examined by light microscopy (BIOREVO BZ-9000, Keyence, Osaka, Japan).

2.3.2. Space maintenance ability. Although the scaffold should ideally disappear from the body after a certain period, it must remain *in vivo* at least until tissue regeneration is complete. In this study, we observed a tendency for the thickness of the specimen on the prepared slide to increase as denaturation advanced; thus, the space maintenance ability was scored by using thickness as an index:

Thickness score: TS

(1) The average thickness of three samples = 0 mm. → TS = 1
(2) The average thickness of three samples > 0 mm. → TS = 2 + (Average thickness/1000)

Since no space is identified when TS is below 2, a TS-2 is considered the lowest level required for the scaffold.

Tissue shrinks during the process of preparing a slide. In other words, the thickness of the specimen on the prepared slide becomes thinner than 5 mm even if the prepared slide containing a 5 mm scaffold is made just after being embedded under the skin. Therefore, the thickness of the collagen fiber scaffold 2 weeks after the operation is actually thicker than that on the prepared slide. In this study, space maintenance ability was evaluated based on the thickness of the specimen on a prepared slide.

2.3.3. Biocompatibility. Once the living body recognizes a foreign body, macrophages are dispatched to eliminate the object. However, the macrophages fuse and become a foreign body giant cell in response to a large foreign body. In other words, the presence of a foreign body giant cell indicates that the body has recognized a large foreign body. In this study, the scaffold in which many foreign body giant cells were identified caused a strong inflammatory reaction and could never be used to construct tissue, even if it remained in place 2 weeks after surgery. Therefore, 'the degree of foreign body' of the scaffold is evaluated by the following score.

Biocompatibility score: BS

(1) BS-1: foreign body giant cells are identified around the embedded collagen fiber scaffold.
(2) BS-2: foreign body giant cells are identified around only a portion of the embedded collagen fiber scaffold.
(3) BS-3: a few foreign body giant cells are identified around the embedded collagen fiber scaffold. (Since a foreign-body reaction appeared below BS-3, this is considered the lowest level of biocompatibility.)
(4) BS-4: no foreign body giant cells are identified around the embedded collagen fiber scaffold.

3. Results

Macroscopic and electron microscopic images of the collagen fiber scaffolds were collected. There was no orientation of collagen fibers unless the suspension was cooled from one direction (figures 1(*c*), (*e*)). Cooling from the bottom of the container yielded collagen fibers arranged perpendicular to the cooling surface, and the pore sizes of this scaffold measured 100–300 μm (figures 1(*d*), (*f*)). The infiltration of cells perfusing the scaffold slowed when the collagen fiber was not oriented properly (figure 1(*g*)). This result was the same for all samples processed at 140 °C for 24 h without collagen fiber orientation. On the other hand, infiltration improved when the collagen fiber in the scaffold was oriented in a single direction (figure 1(*h*)). This result was the same for all samples processed at 140 °C for 24 h with collagen fiber orientation.

We evaluated the relationship between manufacturing conditions and the properties of the created collagen fiber scaffold (table 2). Denaturation of the collagen at 140 °C for 6 h produced a collagen fiber scaffold with TS greater than 2 and BS-3 at 2 weeks after implantation. However, denaturation at 140 °C for more than 12 h yielded no biocompatibility (BS-1). 'Impossible to evaluate' indicates that it was impossible to evaluate the collagen fiber scaffold because it

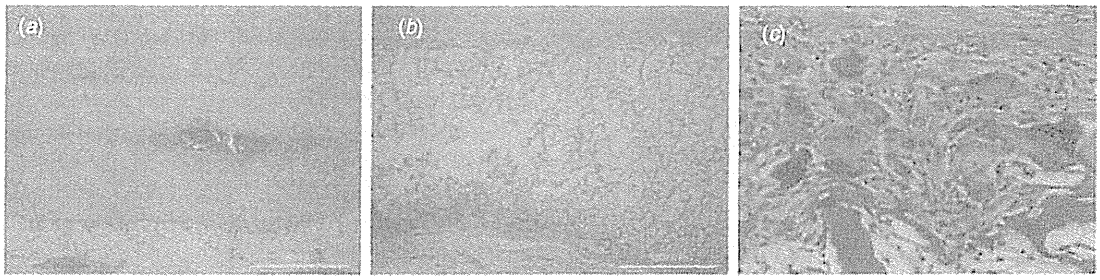

Figure 4. Collagen fiber scaffold with and without thermal denaturation at 140 °C for 24 h, (*a*) collagen fiber scaffold without thermal denaturation after 1 week, (*b*) collagen fiber scaffold with thermal denaturation (140 °C for 24 h) after 2 weeks, (*c*) the foreign body giant cell identified around the scaffold (figure 4(*b*)), the scale bars represent 1000 μm in *a*, *b* and 50 μm in *c*. (H–E image.)

Table 2. Relationship between manufacturing conditions and the properties of the denatured collagen fiber scaffold.

pH	P-temp (°C)[a]	P-time (hours)[b]	Thickness (μm)	Av (μm)[c]	TS[d]	BS[e]
7.4	50	6	0, 0, 0	0	1	IE (3)[f]
7.4	100	6	0, 0, 0	0	1	IE (3)
7.4	100	24	0, 0, 0	0	1	IE (3)
7.4	110	6	0, 0, 0	0	1	IE (3)
7.4	120	6	0, 0, 0	0	1	IE (3)
7.4	120	12	0, 0, 0	0	1	IE (3)
7.4	120	18	0, 0, 0	0	1	IE (3)
7.4	120	24	275, 334, 833	481	2.48	1
7.4	130	6	0, 0, 0	0	1	IE (3)
7.4	140	0	0, 0, 0	0	1	IE (4)
7.4	140	6	701, 827, 1340	956	2.96	3
7.4	140	9	1263, 1571, 1692	1509	3.51	2
7.4	140	12	1215, 1286, 1930	1477	3.48	1
7.4	140	24	1810, 2025, 2286	2040	4.04	1
7.4	170	5	1619, 1691, 2000	1770	3.77	1
7.4	170	6	1691, 2000, 2029	1907	3.91	1

[a] P-temp, processing temperature.
[b] P-time, processing time.
[c] Av, average thickness of 3 samples.
[d] TS, thickness score.
[e] BS, biocompatibility score.
[f] IE, impossible to evaluate.

had disappeared 2 weeks after it was embedded. This indicated insufficient denaturation. The comment noted in the table as 'Impossible to evaluate' was therefore considered to indicate BS-3. However, as for 140 °C for 0 h, it was evaluated as BS-4.

4. Discussion

A collagen microfibril contains five collagen molecules [23–26]; collagen fibrils are formed by aggregation of these microfibrils. Collagen fiber is an assembly of these fibrils. The main epitope of a collagen fiber is in the nonspiral structural telopeptides at both ends of the collagen molecule, and the remainder of the molecule differs little between animal classes.

The collagen used in this experiment is atelocollagen, which is produced by the elimination of the antigenic telopeptides by pepsin. The biocompatibility of atelocollagen without denaturation is very high because BS is 4 at 1 week after embedding. However, there is poor infiltration of cells because spaces for tissue regeneration are not maintained (figure 4(*a*)). Moreover, it was nearly dissolved 2 weeks after embedding. On the other hand, although the mechanical strength increased and sufficient space was maintained even 2 weeks after the operation, antigenicity of the collagen fiber scaffold increased and tissue construction could not be identified when thermal processing was performed at 140 °C for 24 h. Therefore, the collagen fiber scaffold was recognized as a foreign body with low biocompatibility (figure 4(*b*)). This resulted in a foreign body giant cell with multiple nuclei surrounding the scaffold (figure 4(*c*)). Thus, mechanical strength was inversely proportional to biocompatibility. It is thought that optimal 'weak denaturation' occurs at a processing temperature of 140 °C between 0 and 24 h; we concluded the optimal time was 6 h (figure 5(*a*)). Figure 5(*a*) is drawn based on the results of three samples at 140 °C for 0, 6, 9, 12 and 24 h (shown in table 2). Figure 5(*a*) illustrates that although biocompatibility is good, the space maintenance ability is inferior when processing time is shorter than 6 h. On the other hand, the space maintenance ability is superior, but biocompatibility declines when the processing time is longer than 6 h. Since collagen denaturation progresses over time [27], the BS curve shown in figure 5(*a*) declined even if the BS score was the same. The graph accurately reflected the properties of the collagen fiber scaffold indicated in table 2.

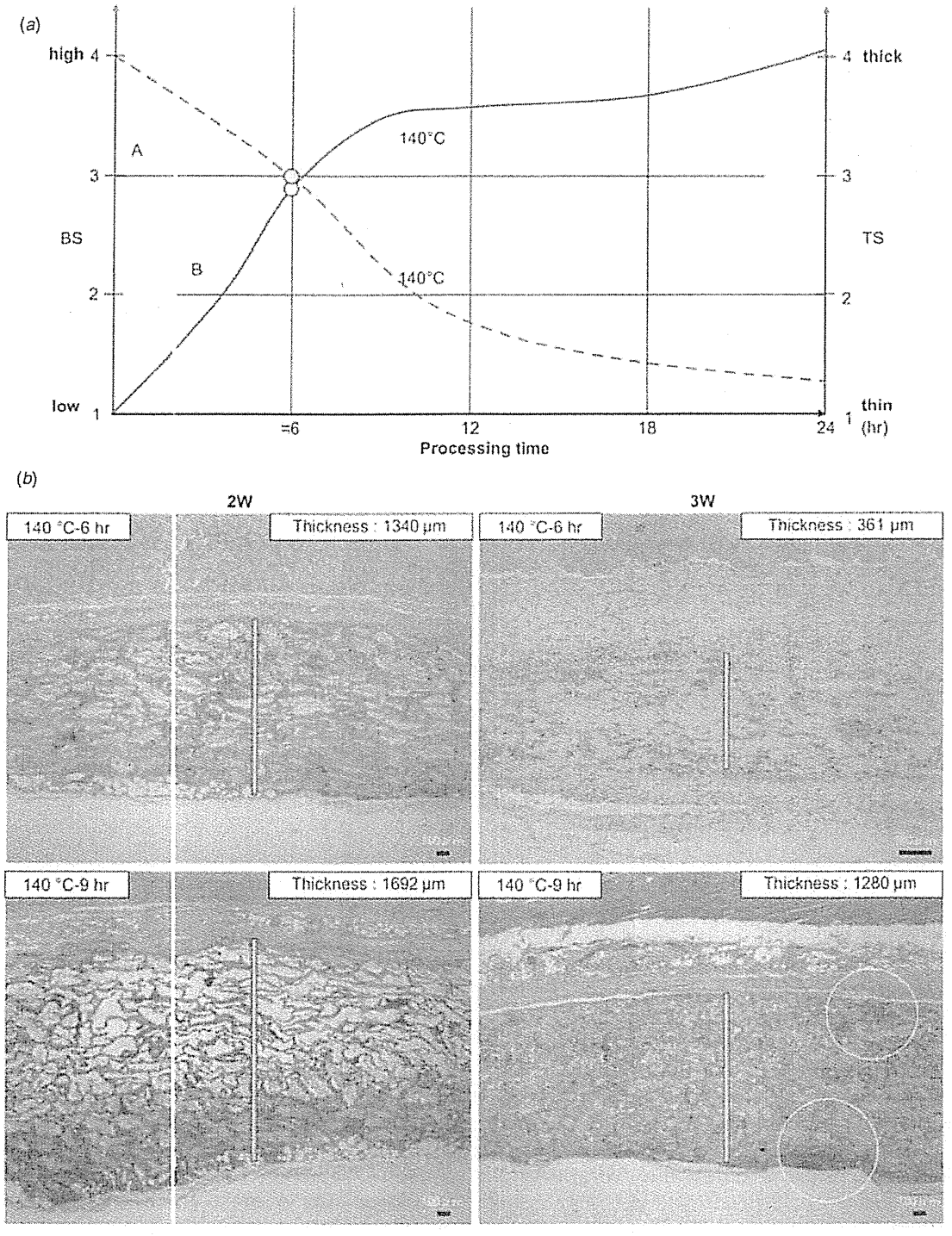

Figure 5. Relationship between thermal denaturation processing time and the space maintenance ability and biocompatibility of a collagen fiber scaffold: (*a*) the red dashed line represents biocompatibility, and the blue line represents space maintenance ability. Line A represents the lowest level of biocompatibility (BS-3) and line B represents the lowest level of space maintenance ability (TS-2) required for the scaffold. (*b*) Thermal denaturation conditions are indicated on the left of each figure and scaffold thickness is indicated on the right. The yellow vertical line in each figure indicates the thickness of each scaffold. The part yellow circled indicates sites of inflammatory cell infiltration. The scale bars represent 100 μm. (H–E image.)

Cells infiltrate the collagen fiber scaffold along collagen fibers; thus, the infiltration rate improved when the scaffold with collagen fiber orientation was used. This is likely because continuous holes are made in the scaffold. This improvement is also likely to ease neovascularity. It is important to ensure blood flow around the region of tissue regeneration to maintain the infiltrated cells. Moreover, when a collagen fiber scaffold containing disseminated cells is implanted, neovascularity in

the early phase is also required to maintain the viability of the disseminated cells. Therefore, orientation of the collagen fibers in a scaffold should improve tissue regeneration. Particularly in the case of hard biomaterials used for bone regeneration, continuous holes greatly improve cell infiltration [28, 29]. Bone tissue engineering reports have suggested the utility of a complex of collagen and glycosaminoglycan (GAG). Tierney *et al* reported that a scaffold with suitable mechanical and biological properties was produced by treatment at 150 °C for 48 h [30] and Haugh *et al* reported scaffolds treated at 150 °C for 120 h or 180 °C for 24 h [31]. The results of both thermal processing methods are far stronger than our results. However, we also found that strong thermal processing at 140 °C for 24 h is suitable for producing a collagen scaffold with the desired mechanical properties. Drexler *et al* used the dehydrothermal cross-linking method and reported that thermal processing at 140°C for 24 h improved mechanical properties and biostability [17]. However, these reports utilized collagen molecules under acidic conditions. Since the properties of collagen molecules are different from those of the collagen fibers used in this study, it is difficult to compare the thermal processing conditions mentioned by Drexler *et al* with the thermal processing condition used in this study (140 °C for 6 h).

Pore size can be controlled by freezing temperature; it becomes smaller as the freezing temperature decreases. Although we made a weakly denatured collagen fiber scaffold by freezing at −80 °C [32, 33], the pore sizes were small and few cells infiltrated the scaffold. Since the pore sizes of the present scaffold measured from 100 to 300 μm, freezing at −10 °C is considered suitable for cell infiltration.

Although the results of this study demonstrated that the most suitable denaturation condition is 140 °C for 6 h, it is possible to apply 140 °C for 5 h for tissue regeneration, as shown in figure 5(*a*). Under these conditions, biocompatibility is slightly improved, while space maintenance ability decreases.

When the scaffolds manufactured under 140 °C for 6 h and 140 °C for 9 h conditions were evaluated at 2 and 3 weeks after the operation, the longer treated scaffold had a greater thickness, while the more briefly heated scaffold demonstrated better biocompatibility, a difference that increased by 3 weeks. Inflammatory cell infiltration was identified in scaffolds processed at 140 °C for 9 h as soon as 3 weeks after operation (figure 5(*b*)). This is consistent with the trend demonstrated in figure 5(*a*).

The results of denaturation at 100 °C and 120 °C are shown in figure 6. The TS at 100 °C for 6 h and 24 h are 1 and the BS at 100 °C for 6 h and 24 h are 3. Since 100 °C is below the denaturation temperature, the line indicating BS is considered almost parallel to the horizontal axis. Denaturation at 120 °C for 18 to less than 24 h (time x) also yielded a scaffold with space maintenance ability and biocompatibility. Therefore, other manufacturing conditions may produce an adequate scaffold. In a previous study, we noted that although the scaffold processed at 120 °C for 24 h was always present even 2 weeks after the operation, the scaffold processed at 120 °C for 23 h was not present in about 50% of cases

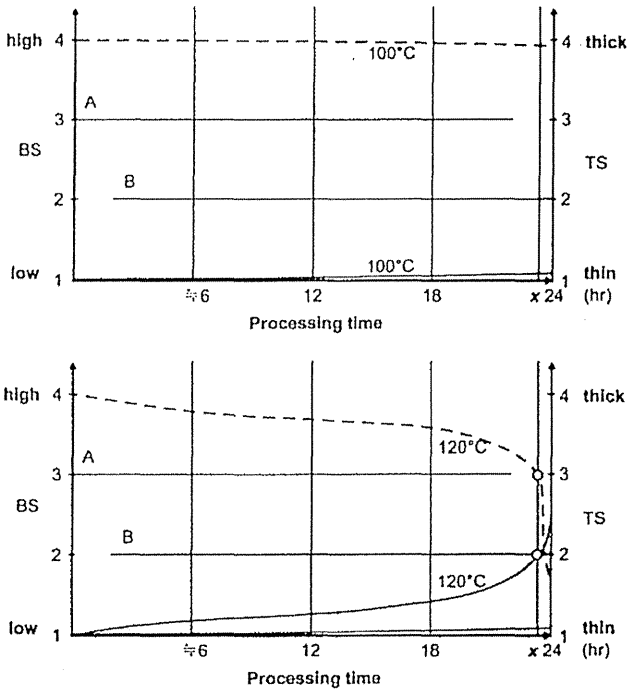

Figure 6. Relationship between thermal denaturation times and the space maintenance ability and biocompatibility of the collagen fiber scaffold. The red dashed line represents biocompatibility, and the blue line represents space maintenance ability. Line A represents the lowest level of biocompatibility (BS-3) and line B represents the lowest level of space maintenance ability (TS-2) required for the scaffold. Time, x, indicates processing time when the denaturation temperature was 120 °C, suggesting that the scaffold is similar to that made at 140 °C for 6 h.

($n = 6$). We believe that the scaffold should remain in place for at least 2 weeks in order to effectively function as a scaffold, so a TS at 120 °C for 23 h is considered to be '1'. Therefore, the time, x, should be between 23 h and 24 h.

A similar experiment is underway using a 6% weakly denatured collagen fiber scaffold. Although the BS was 3, like that of the 3% weakly denatured collagen fiber scaffold 2 weeks after embedding, cells infiltration was poor. This was because the high viscosity of the 6% collagen fiber suspension made it difficult to orient the collagen fibers. In addition, partition of the denatured collagen fiber is thick. A 6% collagen scaffold with orientation can be made occasionally. In such cases, cells infiltrate even to the center of the scaffold along the collagen fiber 2 weeks after the operation. However, few cells' infiltration can be identified in scaffolds without orientation. Therefore, orientation becomes more important when the viscosity is high.

Future experiments will investigate the optimal scaffold strength for specific organs, while reducing the density of the collagen fiber suspension to 6% or less. The shape of our scaffold remains smooth if it is pressed on a plate under conditions at which water is being fully absorbed. Although almost all collagen scaffold materials are made from collagen molecules under acidic conditions, this property is not apparent in acidic collagen scaffolds, including the ones examined in our previous study. The recovery of the scaffold's smooth surface

may contribute to space maintenance for tissue regeneration *in vivo*. Moreover, our scaffold is easily infiltrated with cells if it is pressed several times in cell suspension. This property is useful in the field of cell transplantation [34]. Recently, research efforts to develop a tissue with a three-dimensional structure *in vitro* have been rapidly advancing, and the collagen scaffold developed in this study will be a useful material in various fields.

5. Conclusions

We concluded that collagen denaturation at 140 °C for 6 h produced a scaffold for tissue regeneration with superior space maintenance ability and biocompatibility. Moreover, we suggest that orientation of the collagen fiber in the scaffold facilitates cell infiltration. The concentration of collagen fiber suspension was 3% w/v in this study, but it is possible to control the mechanical strength or the period the scaffold remains *in vivo* by changing the concentration. However, further studies will be necessary to elucidate these conditions. By repeating this process, we think the most suitable scaffold can be produced for any given purpose.

Acknowledgments

We thank T. Miura (Department of Anatomy and Developmental Biology, Kyoto University Graduate School of Medicine, Japan) for investigating cell affinity to the scaffold and T. Ueda (a member of the T. Kawai laboratory, Department of Robotics Osaka Institute of Technology, Japan) for valuable assistance in evaluating sample quality.

References

[1] Akita S, Akino K, Hirano A, Ohtsuru A and Yamashita S 2010 Noncultured autologous adipose-derived stem cells therapy for chronic radiation injury *Stem Cells Int.* **2010** 532704

[2] Bushnell B D, McWilliams A D, Whitener G B and Messer T M 2008 Early clinical experience with collagen nerve tubes in digital nerve repair *J Hand Surg. Am.* **33** 1081–7

[3] Kato Y, Matsumoto I, Tomita S and Watanabe G 2009 A novel technique to prevent intra-operative pneumothorax in awake coronary artery bypass grafting: biomaterial neo-pleura *Eur J Cardiothorac Surg.* **35** 37–41

[4] Ueda K, Tanaka T, Li T S, Tanaka N and Hamano K 2010 Sutureless pneumostasis using bioabsorbable mesh and glue during major lung resection for cancer: who are the best candidates? *J. Thorac. Cardiovasc. Surg.* **139** 600–5

[5] Waitayawinyu T, Parisi D M, Miller B, Luria S, Morton H J, Chin S H and Trumble T E 2007 A comparison of polyglycolic acid versus type 1 collagen bioabsorbable nerve conduits in a rat model: an alternative to autografting *J. Hand Surg. Am.* **32** 1521–9

[6] Inada Y, Morimoto S, Takakura Y and Nakamura T 2004 Regeneration of peripheral nerve gaps with a polyglycolic acid-collagen tube *Neurosurgery* **55** 640–8

[7] Seo K, Inada Y, Terumitsu M, Nakamura T, Horiuchi K, Inada I and Someya G 2008 One year outcome of damaged lingual nerve repair using a PGA-collagen tube: a case report *J. Oral Maxillofac. Surg.* **66** 1481–4

[8] Ignatius A A and Claes L E 1996 *In vitro* biocompatibility of bioresorbable polymers: poly(L, DL-lactide) and poly(L-lactide-co-glycolide) *Biomaterials* **17** 831–9

[9] Suganuma J and Alexander H 1993 Biological response of intramedullary bone to poly-L-lactic acid *J. Appl. Biomater.* **4** 13–27

[10] Nakamura T, Suzuki K, Mochizuki T, Ohde Y, Kobayashi H and Toyoda F 2010 An evaluation of the surgical morbidity of polyglycolic acid felt in pulmonary resections *Surg. Today* **40** 734–7

[11] Lee H, Yeo M, Ahn S, Kang D O, Jang C H, Park G M and Kim G H 2011 Designed hybrid scaffolds consisting of polycaprolactone microstrands and electrospun collagen-nanofibers for bone tissue regeneration *J. Biomed. Mater. Res. B: Appl. Biomater.* **97** 263–70

[12] Powell H M and Boyce S T 2009 Engineered human skin fabricated using electrospun collagen-PCL blends: morphogenesis and mechanical properties *Tissue Eng.* A **15** 2177–87

[13] Lu Q, Zhang S, Hu K, Feng Q, Cao C and Cui F 2007 Cytocompatibility and blood compatibility of multifunctional fibroin/collagen/heparin scaffolds *Biomaterials* **28** 2306–13

[14] Ma L, Gao C, Mao Z, Zhou J and Shen J 2004 Enhanced biological stability of collagen porous scaffolds by using amino acids as novel cross-linking bridges *Biomaterials* **25** 2997–3004

[15] Khor E 1997 Methods for the treatment of collagenous tissues for bioprostheses *Biomaterials* **18** 95–105

[16] Torres-Giner S, Gimeno-Alcaniz J V, Ocio M J and Lagaron J M 2009 Comparative performance of electrospun collagen nanofibers cross-linked by means of different methods *ACS Appl. Mater. Interfaces* **1** 218–23

[17] Drexler J W and Powell H M 2010 DHT crosslinking of electrospun collagen *Tissue Eng. C Methods* **17** 9–17

[18] Sobol E *et al* 2000 Laser reshaping of cartilage *Biotechnol. Genet. Eng. Rev.* **17** 553–78

[19] Gorham S D, Light N D, Diamond A M, Willins M J, Bailey A J, Wess T J and Leslie N J 1992 Effect of chemical modifications on the susceptibility of collagen to proteolysis. II: dehydrothermal crosslinking *Int. J. Biol. Macromol.* **14** 129–38

[20] Weadock K, Olson R M and Silver F H 1983 Evaluation of collagen crosslinking techniques *Biomater. Med. Devices Artif. Organs* **11** 293–318

[21] Koide M, Osaki K, Konishi J, Oyamada K, Katakura T, Takahashi A and Yoshizato K 1993 A new type of biomaterial for artificial skin: dehydrothermally cross-linked composites of fibrillar and denatured collagens *J. Biomed. Mater. Res.* **27** 79–87

[22] Wang M C, Pins G D and Silver F H 1994 Collagen fibres with improved strength for the repair of soft tissue injuries *Biomaterials* **15** 507–12

[23] Gautieri A, Vesentini S, Redaelli A and Buehler M J 2011 Hierarchical structure and nanomechanics of collagen microfibrils from the atomistic scale up *Nano Lett.* **11** 757–66

[24] Moeller H D, Bosch U and Decker B 1995 Collagen fibril diameter distribution in patellar tendon autografts after posterior cruciate ligament reconstruction in sheep: changes over time *J. Anat.* **187** (Pt 1) 161–7

[25] Orgel J P, Irving T C, Miller A and Wess T J 2006 Microfibrillar structure of type I collagen *in situ Proc. Natl Acad. Sci. USA* **103** 9001–5

[26] King G, Brown E M and Chen J M 1996 Computer model of a bovine type I collagen microfibril *Protein Eng.* **9** 43–9

[27] Ueda H, Nakamura T, Yamamoto M, Nagata N, Fukuda S, Tabata Y and Shimizu Y 2003 Repairing of rabbit skull defect by dehydrothermally crosslinked collagen sponges

incorporating transforming growth factor beta1 *J. Control. Release* **88** 55–64

[28] Hamada H, Ohshima H, Ito A, Higuchi W I and Otsuka M 2010 Effect of geometrical structure on the biodegradation of a three-dimensionally perforated porous apatite/collagen composite bone cell scaffold *Biol. Pharm. Bull.* **33** 1228–32

[29] Lee K W, Wang S, Dadsetan M, Yaszemski M J and Lu L 2010 Enhanced cell ingrowth and proliferation through three-dimensional nanocomposite scaffolds with controlled pore structures *Biomacromolecules* **11** 682–9

[30] Tierney C M, Haugh M G, Liedl J, Mulcahy F, Hayes B and O'Brien F J 2009 The effects of collagen concentration and crosslink density on the biological, structural and mechanical properties of collagen-GAG scaffolds for bone tissue engineering *J. Mech. Behav. Biomed. Mater.* **2** 202–9

[31] Haugh M G, Jaasma M J and O'Brien F J 2009 The effect of dehydrothermal treatment on the mechanical and structural properties of collagen-GAG scaffolds *J. Biomed. Mater. Res.* A **89** 363–9

[32] Choi J S, Yang H J, Kim B S, Kim J D, Lee S H, Lee E K, Park K, Cho Y W and Lee H Y 2010 Fabrication of porous extracellular matrix scaffolds from human adipose tissue *Tissue Eng. C Methods* **16** 387–96

[33] Guan J, Stankus J J and Wagner W R 2006 Development of composite porous scaffolds based on collagen and biodegradable poly(ester urethane)urea *Cell Transplant.* **15** (Suppl 1) S17–27

[34] Kempf M, Miyamura Y, Liu P Y, Chen A C, Nakamura H, Shimizu H, Tabata Y, Kimble R M and McMillan J R 2011 A denatured collagen microfiber scaffold seeded with human fibroblasts and keratinocytes for skin grafting *Biomaterials* **32** 4782–92

わが国の臨床研究の現状と未来

Clinical research in Japan——Now and future

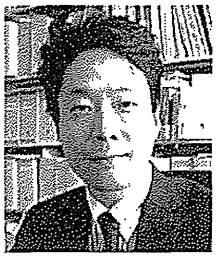

川上浩司
Koji KAWAKAMI
京都大学大学院医学研究科薬剤疫学

◎一口に臨床研究といっても，そのめざすところは多様である．臨床研究には，新医療開発のためのトランスレーショナル研究，臨床現場におけるクリニカルクエスチョンに仮説を立てて検証し，ひいてはエビデンスに基づく医療を実践するための臨床疫学研究，薬剤疫学などの範疇で，医療や薬剤の費用対効果を測定する比較効用性研究，患者個人に対する治療の選定にもかかる患者中心アウトカム研究など，すべてが重要な臨床研究の領域となっている．本稿では，これらについて世界および日本の動向を概説する．

Key word：臨床疫学，薬剤疫学，トランスレーショナルリサーチ，ヘルステクノロジーアセスメント，比較効用性研究

臨床研究における3つの柱

臨床研究には，①新規の医薬品や医療機器の開発にかかる臨床試験，すなわち，トランスレーショナル研究といわれる探索的臨床試験や医薬品の大規模な検証的臨床試験，②臨床現場における自らの診療上の疑問を明らかにするために観察研究や介入研究のデザインで研究を実施し，その結果を診療ガイドラインの改訂に反映させてエビデンスに基づいた医療(evidence-based medicine：EBM)へとつなげるための臨床疫学研究，そして，③診療情報，支払情報，調剤情報，生体情報などのデータベースを利・活用し，薬剤疫学や臨床疫学の手法で観察研究を行い，費用対効果を含む比較効用性研究なども踏まえてあらたな知見を得て社会における医療の受容を勘案し，また基礎研究の道しるべともするための臨床研究といった領域が存在する(図1)．

本稿では，日本における臨床研究の現状をこれらの領域別に考察し，将来に向けて必要な整備について提案する．

医薬品や医療機器開発にかかる臨床試験

現在の日本の薬事法は，医薬品などを繰り返して製造し，国内において販売・流通させるという製造販売業を規制している．それゆえ，規制の対象は大学等研究機関ではなく，営利企業(製薬企業)となっている．薬事法の規定内で，国(厚生労働大臣)からの承認を受けることを目的とした臨床試験は“治験”とよばれており，承認後は薬価収載されて国内の医療機関での当該医薬品の使用が可能となる．この場合，臨床試験(治験)の実施，および治験終了後には，独立行政法人医薬品医療

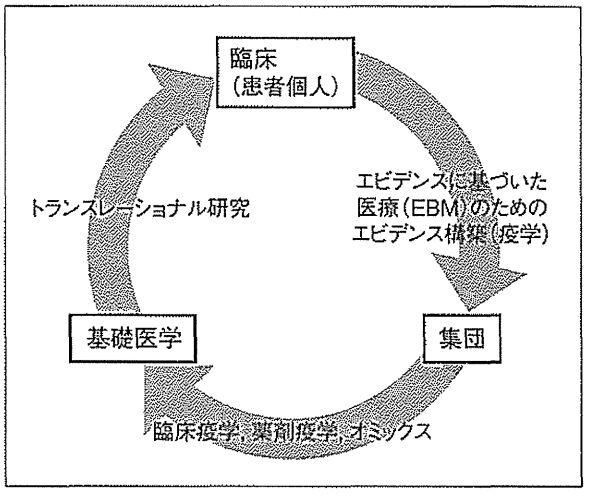

図1　臨床研究のサイクル

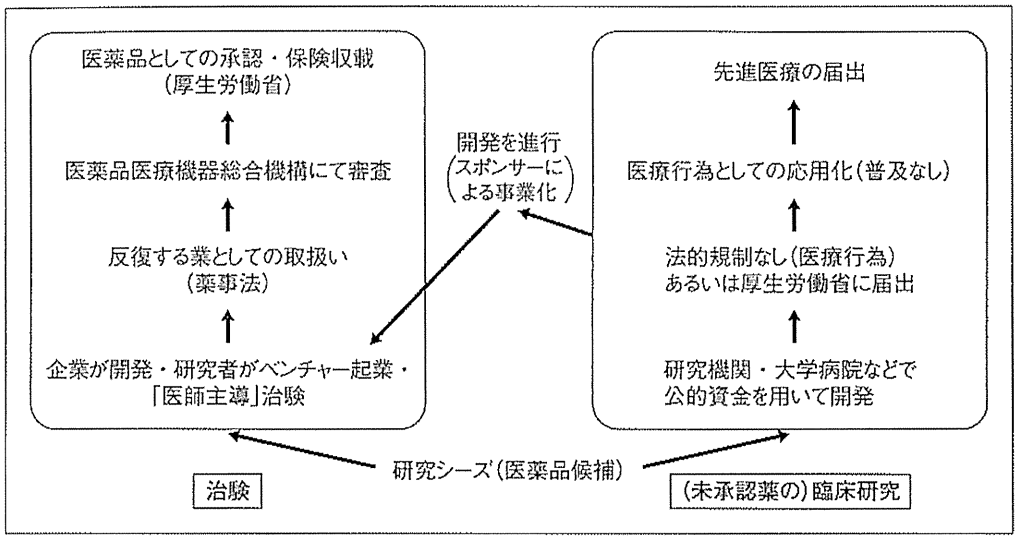

図 2　わが国における臨床試験の現状

機器総合機構(Pharmaceuticals and Medical Devices Agency：PMDA)での審査を経ることになっている．現在では，企業のみならず大学病院などの医療機関が医師主導治験としてPMDAに届出と審査を求めることもできるようになった．

しかし，未承認の新規有効成分であっても，薬事法外の医療行為で大学などが“臨床研究”として実施する場合には，遺伝子・細胞治療品目以外は行政への届出や審査は受けない(図2)．“臨床研究”として，治験ではなく開発を行った場合のゴールは，先進医療のように特定療養費制度のもとで当該医療施設だけで国からの医療費が受けられるというものになる．この臨床研究を実施するためには，臨床研究の倫理指針を遵守する必要はあるが，実施要件にgood clinical practice(GCP)は課せられていないために，実施ハードルは低い．その代わり，得られた臨床データは，科学的品質が担保されているとはみなされず，日本あるいは諸外国の行政当局における医薬品としての承認審査に使用することはできない．

治験と(未承認薬を用いた)臨床研究というダブルトラックの存在は，研究機関における混乱や，近年の臨床研究倫理指針の改正によって改善されたものの，被験者保護の観点，臨床試験の国内統一データベースの不備といった問題を抱えている．しかし，最大の問題は，臨床研究として新規医薬候補品の臨床試験を実施しても，通常その臨床データは国内外の行政当局からはGCPに則る科学的データとはみなされず，以後開発の進行のためにはその後で治験を実施し直さなければならないということである．

そこで，アメリカが運用しているInvestigational New Drug(IND)制度を日本の現状に即して運用できるように，大学などの研究機関で活発に実施される臨床研究を国際水準であるICH-GCPで実施することによって，またその支援を規制当局が行うことによって，シームレスにその成果をフェイズⅡ，フェイズⅢといった企業主体の臨床試験(あるいは治験)へと繋いで，特許期間をむだにすることなく，すこしでも早く医学研究の成果を社会還元，市場導入することが肝要である．昨今，厚生労働省が，臨床研究をICH-GCP水準で実施できるような整備(臨床研究中核病院)を実施している．この推進がひいては日本版INDによる医療開発の促進につながることを期待したい．

エビデンスに基づく医療のための臨床疫学

臨床現場におけるクリニカルクエスチョンについて，何らかの仮説を立てて，それを検証していく研究が臨床疫学研究である．臨床疫学という手法自体は，臨床試験の計画策定などにも重要な手法であるが，なんといってもEBMのためのエビデンスの測定に用いられる手法としての意義が大

きい．エビデンスレベルは，低いものから有識者の意見，症例研究，観察研究，治療法などの介入を伴う臨床試験の結果の順に高いものとなり，査読学術雑誌に掲載された複数の臨床試験の結果から統合レビュー(システマティックレビュー)を実施し，どのような患者層にどのような医療が適切であるかを評価するという手法がもっとも高いエビデンスとされる．近年，このようなエビデンスレベルは，各種の疾病の診療ガイドラインにおいて推奨レベルとして反映されるようになった．

医療の進展の課程において，ある治療法がどの患者のどのような状況で有用なのかを観察研究によって評価し，そこで得られた仮説をもとに当該治療法を介入とした新規の臨床研究計画を策定し，ランダム化比較試験(randomized control trial：RCT)を実施する．それらの集積によりエビデンスレベルの高い結論が得られるわけである．このような流れのなかでは，診療情報を臨床研究に使用することができるような仕組みの整備，レセプト情報や薬剤調剤情報，DPCデータなどのデータベースを活用して，観察研究を推進するための基盤整備，臨床試験の各種薬事規制への理解など，学問としての臨床疫学や薬剤疫学のみならず，多くの周辺領域の振興も必要である．

なお，気をつけなければならないのは，昨今指摘されているEBMの限界である．そもそもエビデンスとは，患者個人個人ではなく，個人を集積した集団を対象として，さまざまな解析を行うものである．しかし，たとえば図3のように既存薬剤aに比べて新規の薬剤bが比較臨床試験の結果，統計学的に優位に有効であることを証明して，薬事承認されて診療ガイドラインにおいて推奨の記載がなされたとしても，その比較はあくまでも集団(この例では中央値どうし)に対して行われるものであり，既存薬剤aに対しての反応が新規の薬剤bに対する反応に比べて良好な患者層も少なからず存在する可能性がある(有効性の逆転)．ということは，臨床医にとっては，自分が診療すべき目の前にいる患者は診療ガイドラインでの推奨どおりに投薬することが本当に正しいのか悩ましいことになる．今後は，診療の前に患者に対して適切な治療法を行うために，オミックスなどの技術をもとにして患者を峻別するような臨床研究もますます必要となろう．

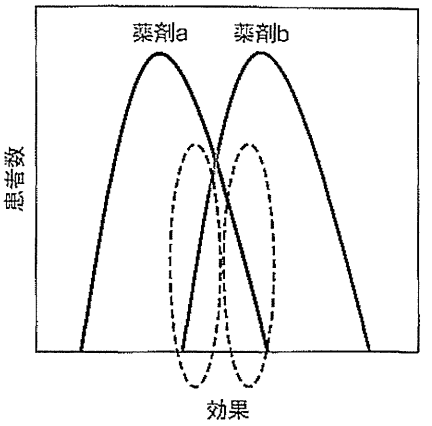

図3　部分集団に対して新薬は必ずしも既存薬よりも効果を示さない

ヘルステクノロジーアセスメントと比較効用性研究

科学技術の成果の社会受容のために，特定の医療費や薬価などが適正かどうかを評価することをヘルステクノロジーアセスメント(以下，HTA)という．HTAには，①EBM，②費用便益分析(cost benefit analysis：CBA)，③比較効用性研究(comparative effective research：CER)，のプロセスすべてが包含される．EBMの実践のためには，いずれの治療を選択するかという意思決定をするための科学的な根拠を提示する．CBAは医療介入することによるトータルな費用と便益とを分析する．CERは薬剤疫学の領域などで実施されるもので，たとえば，特定の疾患に対する医療行為AとBとが一定の治療効果を有すると仮定した場合，AとBとでいずれのほうがかかる費用に対する効果があるかについて，統計学的手法を用いて解析するというものである．抗癌剤治療などにおいては，患者の生存期間にQOLの観点も合わせた質調整生存年(quality adjusted life year：QALY)や，従来療法よりも1QALY多く得るために必要な追加費用(incremental cost-effectiveness ratio：ICER)といった指標を用いることもある．いずれもリスクとベネフィットのトレードオフに焦点を当てている．

現在，世界的な人口の増加と先進国における社

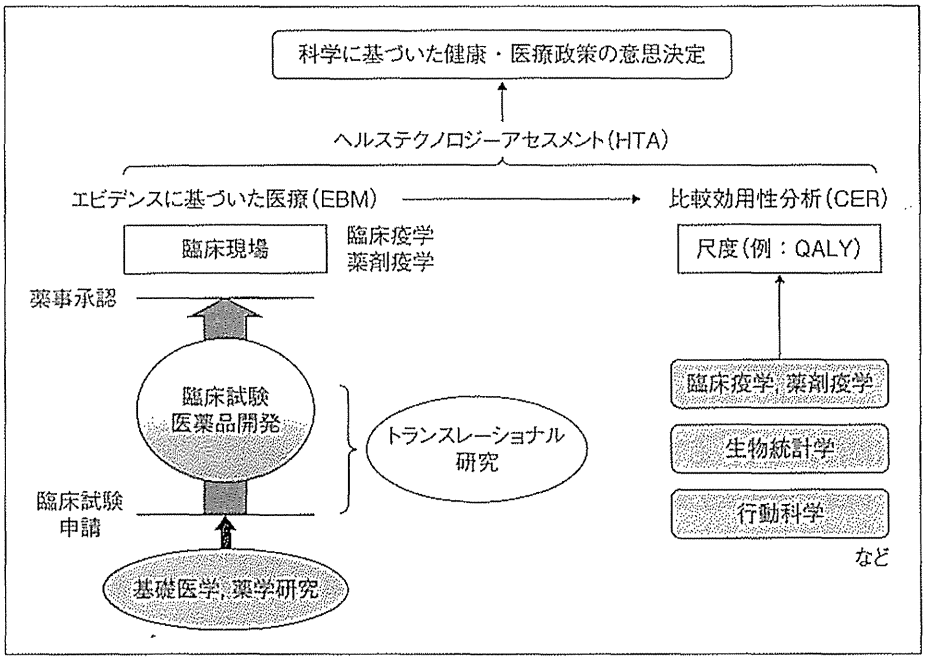

図 4　ヘルステクノロジーアセスメントの概念図

会の高齢化によって，各国ともに医療費の増加にあえいでいる．持続的な社会保障の維持のためには，医療費・薬剤費の適正化，あるいは政策的には削減をせざるをえない局面を迎えている．そこで，さまざまな臨床データをもとに，計量経済学的手法も合わせてCERを実施するようになっている．医療の質を評価して実行するには，EBMのための臨床疫学手法によってエビデンスを測定し，つぎにその費用対効果を評価するCERを実践していくという順序がとられる(図4)．エビデンスを測定した後に，たとえば2つの異なる治療法が存在し安全性・有効性の等しい場合，どちらがある疾患の治療に対して費用対効果がよいのかを評価するために，臨床状態を系統樹として設定するマルコフ推移モデルを作成し，その後に推移確率を代入し，モンテカルロシミュレーションといった疫学・生物統計学的手法を用いて，CERが実施されるのである．

1990年代後半から，ヨーロッパ，アメリカ，アジア諸国において，各国政府にHTAを実践する独立機関が設立された．昨今，アメリカにおいては，HTA機関である医療研究品質評価庁(Agency for Healthcare Research and Quality：AHRQ)のみならず，医薬品などの許認可によってレギュラトリーサイエンスを実践する食品医薬品庁(Food and Drug Administration：FDA)もCERの重要性を訴えるようになっている．一方，日本においては，まだHTAの組織的研究は萌芽的であり，政府機関もいまだ存在していないが，昨今，厚生労働省に医療の費用対効果を検討する部署と取組みがはじまったところである．

個別化医療に向けた臨床研究の今後の方向性

『*N. Engl. J. Med.*』の2012年10月25日号においては，964例の大腸癌あるいは直腸癌患者においてphosphatidylinositol 3-kinase(PI3K)の触媒サブユニットをコードする*PIK3CA*遺伝子の変異がアジュバント使用でのアスピリンの効果に影響するという分子疫学研究が報告された[1]．*PIK3CA*遺伝子に変異のある大腸癌患者に診断後アスピリンが投与されている場合，大腸癌特異的死亡が82%も減少したのである．*PIK3CA*遺伝子に変異のない場合には，アスピリン投与は生存に影響を与えなかった．この研究において，*PIK3CA*遺伝子をバイオマーカーとして使用することで，アスピリン投与の大腸癌の治療上の便益を予測できることになる．この作用機序として

は，大腸癌における *PIK3CA* 遺伝子の変異はPTGS2を活性化することで大腸癌細胞のアポトーシスを抑制しているために，アスピリン投与がその抑制解除に働くことによると考えられている．

ステージⅢの大腸癌の術後療法においては，分子標的薬を含むあらゆる抗癌剤においても，臨床試験でこの10年余りの間，予後延長を示すことができなかった．2009年に大腸癌の診断後のアスピリン投与で29%の大腸癌関連死を減少させ，サブ解析においてはPTGS2(cyclooxygenase-2)を高発現する腫瘍においてとくに顕著に減少効果があるという報告[2]があった後，イギリスにおける5つの臨床試験からのメタアナリシスにおいて，アスピリンが心血管イベントを抑制する効果があるという報告のなかで，大腸癌患者においては74%の転移リスク減少があるという知見[3]もあり，昨今アスピリンの効果に対する関心が高まっているところである．

本稿はまだ症例数も少なく萌芽的な解析となっていることは否定できないが，*PIK3CA* 遺伝子の変異は初発大腸癌の1/6以上にみられるため，分子疫学の進歩が疾患治療のためのバイオマーカーの同定に寄与していくことで，非常に古くから用いられており，安価な医薬品であるアスピリンが，21世紀の標的治療として脚光を浴びるという新しい可能性を示唆しているのである．

おわりに

本稿では，トランスレーショナル研究，臨床疫学研究，比較効用性研究の3つの軸を中心に，患者個人に対する治療の選定にもかかるような，患者中心アウトカム研究(Patient Centered Outcomes Research：PCOR)ともいうべきあらたな臨床研究の可能性についても言及した．将来に向けて，日本の大学医学部は，これまでの臨床医学，基礎医学という2つの考え方のみならず，臨床研究に関する教育カリキュラムの開発と教員・学生の育成，そしてその実践の基盤構築を真剣に考えるべきである．とくに，日本においてきわめて基盤の弱い社会医学の領域は，臨床研究教育にはなくてはならないものである．今後，日本の医学のパラダイムを変えていき，臨床研究が多様性をもって力強く推進していくことを願ってやまない．

文献

1) Liao, X. et al.: *N. Engl. J. Med.*, **367**：1596-1606, 2012.
2) Chan, A. T. et al.: *JAMA*, **302**：649-658, 2009.
3) Rothwell, P. M. et al.: *Lancet*, **379**：1591-1601, 2012.

*　　*　　*

I. 現在実現化に最も近い，外科領域における再生医療研究

3. 生体内組織再生誘導型の人工気管

Artificial trachea with in situ induction of tissue regeneration

1. 福島県立医科大学医学部耳鼻咽喉科学講座
2. 北野病院耳鼻咽喉科
3. 京都大学再生医科学研究所再生医学応用研究部門臓器再建応用分野

大森　孝一[1]・多田　靖宏[1]・野本　幸男[1]・谷　亜希子[1]
Koichi Omori（教授）　*Yasuhiro Tada*（講師）　*Yukio Nomoto*（講師）　*Akiko Tani*
仲江川雄太[1]・金丸　眞一[2]・中村　達雄[3]
Yuta Nakaegawa　*Shin-ichi Kanemaru*（主任部長）　*Tatsuo Nakamura*（准教授）

Summary

気管・輪状軟骨の再建は最も難しい外科治療のひとつである。筆者らは生体内組織再生誘導型の人工気管を開発し，気道としての枠組みを保持するためポリプロピレン製メッシュを管状にし，同素材のリングで補強し，その表面に組織再生の足場として医療用のブタ皮膚由来のコラーゲンスポンジを付着させた。

大型動物への移植実験で最長５年の経過観察で安全性，有効性が確認され，施設内倫理委員会の承認のもと，2002年より筆者らは生体内組織再生誘導型の人工気管を用いた気道の再生医療を世界に先駆けて行っている。甲状腺癌の気管浸潤例に対する気管再建と喉頭気管狭窄例に対する病変切除後の二期的再建を行い，成人11例において最長７年の経過観察で内腔上皮再生が得られている。

生体内組織再生誘導型の人工気管は製造方法が完成しており，製造から販売を取り扱う企業が決まれば医療機器としての実用化が実現し，患者のQOL向上に寄与できるものと思われる。

Surgery Frontier 21(1)：31-35，2014

Key Words　人工気管，生体内組織再生誘導，*in situ* Tissue Engineering

はじめに

気道は鼻腔，口腔，咽頭，喉頭，気管と気管支・細気管支によって構成される。喉頭は呼吸，嚥下，発声という重要な役割をもち，気管は呼気や吸気の通り道であると同時に，線毛運動と咳反射により分泌物や異物を除く排泄路として機能している。

気管や輪状軟骨に悪性腫瘍や狭窄性疾患を生じると，病変の切除後に気道を再建する必要がある[1)]。悪性腫瘍としては甲状腺癌，肺癌などがあり，狭窄性疾患としては内腔からの損傷と外

表１　気管・輪状軟骨再建の主な適応疾患

悪性腫瘍	甲状腺癌，肺癌，気管原発腫瘍
炎症性狭窄	気管内腔からの損傷（気管挿管チューブ，気管カニューレ，熱傷，化学的腐食剤）
	気管外からの損傷（交通外傷，刃物による裂傷，銃創，気管切開術後）
	炎症性疾患（再発性多発軟骨炎，結核）
	特殊な疾患（いわゆるWegener肉芽腫，アミロイドーシス）

◈メモランダム◈

in situ Tissue Engineering ―組織工学の新しいトレンド―

培養室のシャーレのなかで組織や臓器を作る組織工学（Tissue Engineering）は1990年代に始まり夢の技術として注目された。しかしながら，シャーレのなかで作られた組織を体に埋め込むと吸収されるという問題が明らかになった。そこで，再生医療の実用化に向けて，患者の体内の本来の場所で組織を再生させる*in situ* Tissue Engineeringが組織工学の新しいトレンドとして期待を集めている。

からの損傷があり，炎症性疾患もある（表1）。

気管・輪状軟骨を再建する際には，管腔を保持する硬度をもつ枠組みと内腔面に線毛をもつ粘膜を同時に再建することが理想的である。また，喉頭の下部を構成する輪状軟骨は気管より管腔が狭く再狭窄を起こしやすいことから，再建は難しい。これらの課題を解決するために，筆者らは生体内組織再生誘導型の人工気管を開発しており，現在実現化に最も近い，外科領域における再生医療研究として，その開発コンセプトと少数例の臨床経験を紹介する。

従来の気道再建外科

従来の気道再建外科を表2にまとめる。1970年代からGrilloのグループが気管端々吻合術を報告してきたが[2]，広範囲切除の限界，縫合不全や縦隔炎などの重篤な合併症，術後の頸部前屈姿勢など，容易な手術ではない。輪状軟骨切除後の端々吻合術も一部の施設で行われている。1980年代からCottonらにより移植をともなう再建術が報告されており[3]，硬性再建には骨，軟骨が用いられ，内腔面には皮膚や粘膜が用いられるが，自家遊離移植では複数部位や複数回にわたる手術侵襲が必要であるうえに，移植片の移動や吸収の問題があり気道の枠組みとしての長期的安定性を保持するのが難しい。人工材料にはシリコン，チタンなどの材料が用いられてきたが安定した成績を上げていない[4]。悪性腫瘍に対しては，進行甲状腺癌の気管浸潤例では十分な安全域をとった治癒切除が望まれるが，大きく切除すれば再建は難しくなり，自家遊離移植は欠損部の大きさによって制限される。

表2　従来の気道再建外科治療と問題点

	問題点
端々吻合 （気管，輪状軟骨）	縫合不全（吻合部緊張や血流不全），術後管理（長期の頸部前屈）
自己組織移植 （硬性組織として軟骨や骨，複雑な手術操作（複数部位，複数回） 内腔面として皮膚や粘膜）	
人工材料移植 （シリコン，チタン，ポリプロピレンメッシュ）	低い成功率

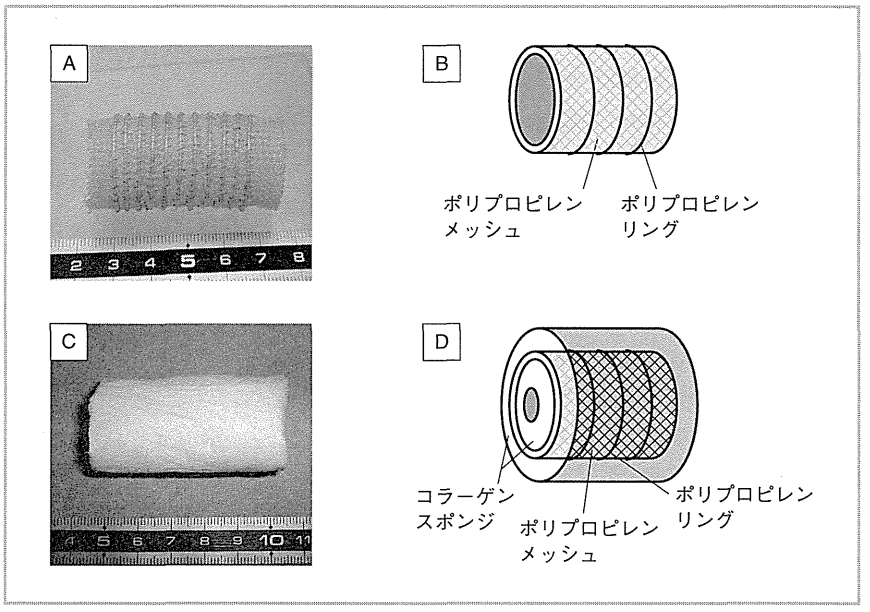

図1　人工気管

A：骨格，B：骨格のシェーマ，C：外観，D：外観のシェーマ

（カラーグラビアp3　写真5参照）

場の理論と生体内組織再生誘導型の人工気管

1993年，LangerとVacantiは体外で細胞を培養して工学的手法により臓器や組織に近いものを再生させる

Tissue Engineeringという概念を提唱したが[5]，体外で作られた組織が体内への移植後に吸収されるなどの問題があり，臨床応用へのハードルは高い。一方，生体内で組織の再生を誘導する手法は*in vivo* Tissue Engineering，生体内の本来の場所で組織の再生を誘導する手法は*in situ* Tissue Engineeringといわれる。

傷害された組織・臓器は，本来，自己再生能力を有しているが，生体組織が大きく欠損した場合や急激な組織修復により組織再生の場が奪われてしまうと，瘢痕化などにより元の組織が再生しない。組織再生の適切な場が適切な組織再生を促進するという考え方を場の理論という。1995年以降，中村らは場の理論に基づいたコンセプトで，コラーゲンスポンジを主体とした足場の移植で気管[6]，食道，胃，小腸，末梢神経などの組織再生を報告した。

生体内組織再生誘導型の人工気管（図1）は[6]，気道としての管状の枠組みを保持するため，ポリプロピレン製メッシュを管状にし，同素材のリングで補強した。ポリプロピレン製メッシュは特定保険材料として従来から胸壁や腹壁の補強に臨床で使われている。ポリプロピレン管の表面に，組織再生の足場としてコラーゲンスポンジをグラフト化，重層コーティングして厚く付着させた。コラーゲンスポンジは医療用のブタ皮膚由来のコラーゲンを用いた。

頸部気管については，イヌの頸部気管を切除した後に人工気管を移植し，最長5年の観察で，気管の上皮再生は

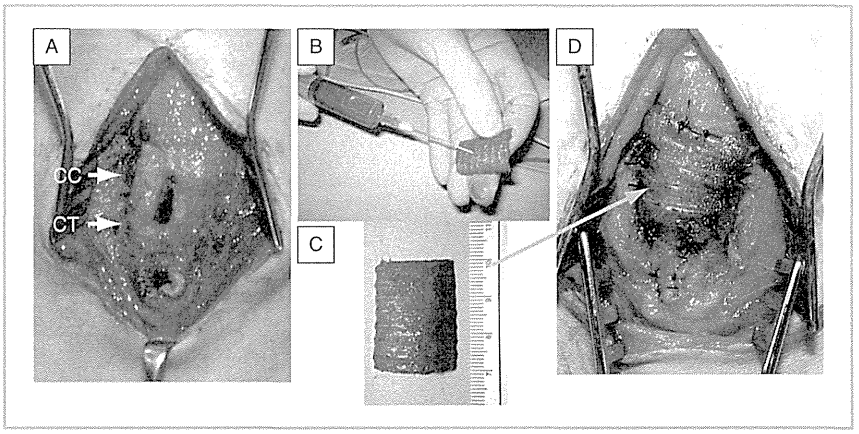

図2　人工気管を用いた再建手術（声門下・頸部気管狭窄例）
A：輪状軟骨（Cricoid Cartilage；CC）・頸部気管（Cervical Trachea；CT）の欠損部
B：人工気管を半周分にトリミングし血液を湿潤
C：移植前の人工気管
D：前壁を被覆するように人工気管を縫合固定　（カラーグラビアp4　写真6参照）

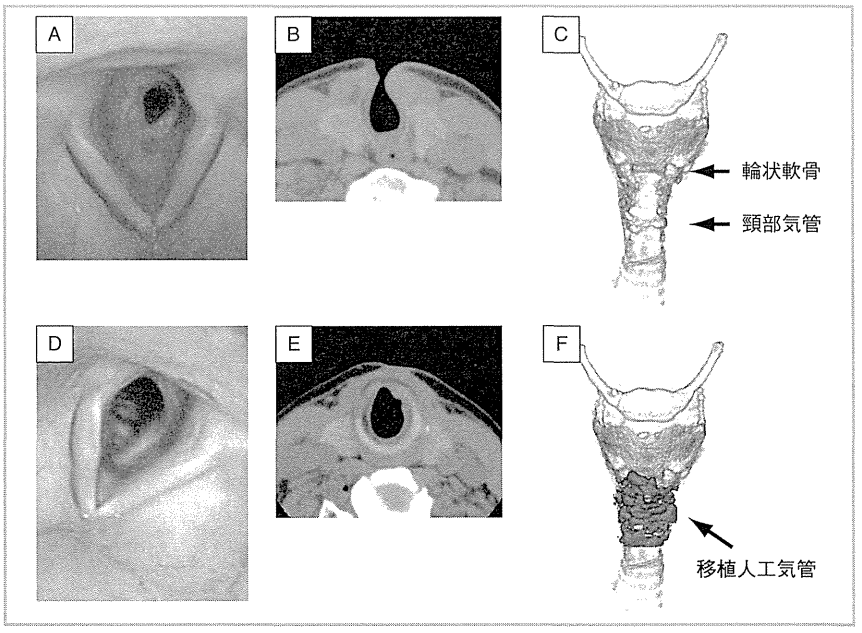

図3　術前術後の画像所見
A：初診時の内視鏡像：声門下の高度狭窄を認め呼吸困難がある。
B：瘢痕切除後，再建術前のCT：気道の内腔は狭小化している。
C：瘢痕切除後，再建術前の3D-CT：輪状軟骨・頸部気管の前壁に欠損を認める。
D：再建術後4年の内視鏡像：内腔面は粘膜に覆われ再狭窄を認めていない。
E：再建術後のCT：気道の内腔は十分保たれている。
F：再建術後の3D-CT：移植人工気管により欠損していた前壁が再建された。
（カラーグラビアp4　写真7参照）

表3　人工気管の実用化を目指した医療機器開発推進研究

・生産ライン構築（GMP/QMS 準拠）
　医療機器製造クリーンルーム
　製造手順書作成
　製造・品質・衛生管理

・生物学的安全性試験（GLP 準拠）

・臨床試験準備
　臨床試験実施手順書の作成

良好で問題なく経過した。組織学的評価では，炎症所見を認めず，内腔面は再生線毛上皮で覆われていた。再生気管の強度は機械的圧縮試験で正常気管と同程度であった。正常気管との接合部も安定した組織移行がみられ，長期に安全に使用できることがわかった[6)7)]。輪状軟骨については，輪状軟骨の弓部を切除した後に人工気管をトリミングして移植し，最長1年の観察で，一部メッシュが露出したが上皮再生は良好で問題なく経過した[8)]。なお，動物の愛護および管理に関する法律および所属施設の動物実験委員会の指針に従って実験を行った。

臨床症例

大型動物への移植実験で最長5年の経過観察で良好な内腔上皮再生が得られ安全性が確認されたことから，施設内倫理委員会の承認のうえ，2002年より筆者らは，生体内組織再生誘導型の人工気管を用いた気道の再生医療を世界に先駆けて行っている。甲状腺癌の気管浸潤例に対する気管再建と喉頭気管狭窄例に対する病変切除後の二期的再建を行い，現在まで経験した成人11例において最長7年の経過観察で内腔上皮再生が得られている[9)-11)]。声門下・頸部気管狭窄例の気道再建手術，内視鏡およびCT所見を図2，図3に示す。

生体内組織再生誘導型の人工気管は，少数の臨床例における最長7年の観察で，頸部気管と輪状軟骨においては安全性，有効性は確認されている。人工気管はトリミングが可能で，欠損部に適した気道再建手術を容易に安定して実施できるとともに，ほかの部位からの組織採取が不要で手術侵襲を軽減させ，患者のQOL向上に寄与できる。

人工気管の製造方法は完成しており，足場のみを用いるため細胞移植に比べると製造管理や品質管理などのハードルは低い。人工気管が一般医療として広く用いられることが期待されており，現在厚生労働省科学研究費の助成を受け，医療機器としての実用化に向けて，製造環境の整備，製造工程の手順書作成，品質管理の精度向上などGMP/QMS準拠の生産ライン構築に取り組んでいる（表3）。今後，製造から販売を取り扱う企業が決まれば，医療機器として実現するものと期待される。

気管の再生医療研究の動向

2002年，Langerらのグループはヒツジの気管再生を試みたが術後の気道閉塞などの問題があり，臨床応用には至っていない[12)]。2008年にはMacchiariniらによりallograftを用いた気管再建が報告され，死体気管の軟骨構造に患者由来の上皮細胞と軟骨細胞を付加して移植したところ，術後4カ月で内腔を保持しており[13)]，2011年には骨髄単核球と人工気管を移植し術後5カ月で内腔を保持していたと報告した[14)]。

筆者らは気管再生の基礎研究として，上皮化を加速するための線維芽細胞や脂肪組織由来幹細胞の付加技術[15)]，ゲル薄膜を用いた人工材料[16)]，声帯隆起の再生に取り組んでいる。将来的には小児例へ適用可能な吸収性材料からなる新規人工気管の開発が望まれる。

おわりに

生体内組織再生誘導型の人工気管は，動物実験で最長5年の観察，その後の少数の臨床例における最長7年の観察で，頸部気管と輪状軟骨については安全性，有効性は確認されている。製造方法は完成しており，足場のみを用いるため細胞移植に比べると製造管理や品質管理などのハードルは低い。現在GMP/QMS準拠の生産ラインを整備しつつあり，製造から販売を取り扱う企業とのマッチングが得られれば医療機器としての実用化が実現し，これにより患者のQOL向上に寄与できるものと思われる。

謝辞

本研究の一部は平成24年度厚生労働科学研究費補助金（医療技術実用化総合研究事業），平成25年度厚生労働科学研究費補助金（医療機器開発推進

研究事業）を受け実施した。

文 献

1）大森孝一：気管の再建．耳喉頭頸 81：118-125，2009
2）Grillo HC：The history of tracheal surgery. Chest Surg Clinics North America 13：175-189, 2003
3）Cotton R：Management of subglottic stenosis. Otolaryngologic Clinics North America 33：111-130, 2000
4）Neville WE, Bolanowski JP, Kotia GG：Clinical experience with the silicone tracheal prosthesis. J Thorac Cardiovasc Surg 99：604-613, 1990
5）Langer R, Vacanti JP：Tissue engineering. Science 260 (5110)：920-926, 1993
6）Teramachi M, Kiyotani T, Takimoto Y, et al：A new porous tracheal prosthesis sealed with collagen sponge. ASIO J 41：306-310, 1995
7）Nakamura T, Teramachi M, Sekine T, et al：Artificial trachea and long term follow-up in carinal reconstruction in dogs. Int J Artificial Organs 23：718-724, 2000
8）Omori K, Nakamura T, Kanemaru S, et al：Cricoid regeneration using in situ tissue engineering in canine larynx for the treatment of subglottic stenosis. Ann Otol Rhinol Laryngol 113：623-627, 2004
9）Omori K, Nakamura T, Kanemaru S, et al：Regenerative medicine of the trachea：The first human case. Ann Otol Rhinol Laryngol 114：429-433, 2005
10）Omori K, Tada Y, Suzuki T, et al：Clinical application of in situ tissue engineering using a scaffolding technique for reconstruction of the larynx and trachea. Ann Otol Rhinol Laryngol 117：673-678, 2008
11）大森孝一，中村達雄，多田靖宏，他：甲状腺癌における気道の再生医療．再生医療 5：89-93，2007
12）Kojima K, Bonassar LJ, Roy AK, et al：Autologous tissue-engineered trachea with sheep nasal chondrocytes. J Thorac Cardiovasc Surg 123：1177-1184, 2002
13）Macchiarini P, Jungebluth P, Go T, et al：Clinical transplantation of a tissue-engineered airway. Lancet 13：372(9655)：2023-2030, 2008
14）Jungebluth P, Alici E, Baiguera S, et al：Tracheobronchial transplantation with a stem-cell-seeded bioartificial nanocomposite：a proof-of-concept study. Lancet 378：1997-2004, 2011
15）Kobayashi K, Suzuki T, Nomoto Y, et al：A tissue-engineered trachea derived from a framed collagen scaffold, gingival fibroblasts and adipose-derived stem cells. Biomaterials 31：4855-4863, 2010
16）Tada Y, Takezawa Y, Suzuki T, et al：Regeneration of tracheal epithelium utilizing a novel bi-potential collagen scaffold. Ann Otol Rhinol Laryngol 117：359-365, 2008

A novel surgical marking system for small peripheral lung nodules based on radio frequency identification technology: Feasibility study in a canine model

Fumitsugu Kojima, MD,[a,b] Toshihiko Sato, MD, PhD,[b] Hiromi Takahata, MEng,[c] Minoru Okada, PhD,[d] Tadao Sugiura, PhD,[d] Osamu Oshiro, PhD,[c] Hiroshi Date, MD, PhD,[b] and Tatsuo Nakamura, MD, PhD[a]

Objective: We investigated the feasibility and accuracy of a novel surgical marking system based on radiofrequency identification (RFID) technology for the localization of small peripheral lung nodules (SPLNs) in a canine model.

Methods: The system consists of 4 components: (1) micro RFID tags (13.56 MHz, 1.0 × 1.0 × 0.8 mm), (2) a tag delivery system with a bronchoscope, (3) a wand-shaped locating probe (10-mm diameter), and (4) a signal processing unit with audio interface. Before the operation, pseudolesions mimicking SPLNs were prepared in 7 dogs by injecting colored collagen. By use of a computed tomographic (CT) guide, an RFID tag was placed via a bronchoscope close to each target lesion. This was then followed by scanning with the locating probe, and wedge resection was performed when possible. Operators can locate the tag by following the sound emitted by the system, which exhibits tone changes according to the tag-probe distance. The primary outcome measure was the rate of wedge resection with good margins.

Results: A total of 10 pseudolesions imitating SPLNs were selected as targets. During thoracoscopic procedures, 9 of 10 tags were detected by the system within a median of 27 seconds. Wedge resections were performed for these 9 lesions with a median margin of 11 mm. The single failure was caused by tag dislocation to the central airway.

Conclusions: Successful localization and wedge resection of pseudolesions with appropriate margins were accomplished in an experimental setting. Our RFID marking system has future applications for accurately locating SPLNs in a clinical setting. (J Thorac Cardiovasc Surg 2014;147:1384-9)

Video clip is available online.

The accurate localization of small peripheral lung nodules (SPLNs) in a thoracoscopic setting is a challenging task, although video-assisted thoracic surgery is a more suitable approach than open surgery for small lesions.[1] In accordance with evolving patient and social demands, the importance of minimally invasive surgical procedures has increased in recent years. In 2010, the rate of video-assisted thoracic surgery reportedly reached nearly 60% of lung cancer surgery in Japan[2] and 44.7% in the United States.[3] The vast majority of SPLNs are therefore likely to be resected by a thoracoscopic approach in Japan.

Many techniques to assist the localization of SPLNs have been developed and reported; these include finger palpation, percutaneous hook-wire placement, preoperative dye marking, fluoroscopy with a contrast medium, intraoperative ultrasonography (US), and radiotracer-guided surgery.[4] These techniques have proved reliable to a certain extent, but all possess considerable problems in complications, cost, technical difficulty, and availability of facilities.[5] Consequently, there is not yet an established "best technique," and the choice of method is highly dependent on each surgeon's preference.

Despite the lack of a definitive solution for determining SPLN location, thoracic surgeons are required to manage an increasing number of small pulmonary nodules owing to the continued improvement of computed tomography (CT) technology. In 2011, the National Lung Screening Trial established the ability of low-dose CT screening to reduce mortality in a high-risk population.[6] Also, recent guidelines for lung cancer screening from The American

From the Department of Bioartificial Organs,[a] Institute for Frontier Medical Sciences, Kyoto University, Kyoto; the Department of Thoracic Surgery,[b] Kyoto University Hospital, Kyoto; the Graduate School of Engineering Science,[c] Osaka University, Toyonaka; and the Graduate School of Information Science,[d] Nara Institute of Science and Technology, Ikoma, Japan.

This project was supported by grants from The Japanese Foundation for Research and Promotion of Endoscopy, and Japan Society for the Promotion of Science Fujita Memorial Fund for Medical Research.

Disclosures: Authors have nothing to disclose with regard to commercial support.

Received for publication March 7, 2013; revisions received May 15, 2013; accepted for publication May 31, 2013; available ahead of print July 15, 2013.

Address for reprints: Toshihiko Sato, MD, PhD, Department of General Thoracic Surgery, Kyoto University, 54 Shogoin, Kyoto 6068507, Japan (E-mail: tsato@kuhp.kyoto-u.ac.jp).

0022-5223/$36.00

http://dx.doi.org/10.1016/j.jtcvs.2013.05.048

ET/BS

Abbreviations and Acronyms
CT = computed tomography
RFID = radiofrequency identification
SPLN = small peripheral lung nodule
US = ultrasonography

Association for Thoracic Surgery have recommended the surgical excision of subcentimeter lesions in patients whose tumors show suspicious changes in size or appearance.[7] For years, the preoperative marking for lung nodules smaller than 10 mm in size has also been recommended.[8] In light of these advances in CT screening and recommendations, there is an unprecedented need to improve localization techniques.

Furthermore, in this era of minimally invasive surgery, there is an increasing demand for innovative localization techniques. An ideal method not only would ensure patient safety but also would allow for adequate minimum margins from the lesion. For instance, maintenance of appropriate margins for sublobar curative resection of primary lung cancer has been shown to reduce recurrences.[9] The importance of appropriate margins has similarly been emphasized in the resection of metastatic pulmonary nodules to prevent local recurrence.[10] However, for surgeons to ensure adequate margins, they must first be able to gauge the exact distance from the target lesion to the cutting line for resection.

To address these problems, we have proposed a novel surgical marking system based on radiofrequency identification (RFID) technology, which provides a precise ranging ability.[11] In our system, 13.56-MHz micro RFID tags are used as "wireless surgical markers" to label lesions that are otherwise difficult to locate. In this study, we test the feasibility and reliability of this RFID marking system using experiments with pseudolesions imitating SPLNs in a canine model.

MATERIAL AND METHODS

RFID Marking System

The schematic diagram of our proposed RFID marking system is shown in Figure 1. The entire system consists of the following 4 main components: (1) micro RFID tags coated with polyester resin (13.56 MHz, 1.0 × 1.0 × 0.8 mm; Star Engineering Co, Ltd, Singapore), (2) tag delivery system with bronchoscope, (3) wand-shaped locating probe (10-mm diameter), and (4) signal processing unit with audio interface.

The detailed composition and algorithms of the system have been reported in our previous article.[11] The micro RFID tag works as a passive transponder without a built-in battery, with the locating probe acting as both a power supply coil and a receiver antenna. When the probe is placed in close proximity to the tag, the tag is activated by the electromagnetic field produced by the probe. The activated tag returns the response signal with a fixed wavelength of 13.56 ± 0.423 MHz. The distance between the probe and the target tag is measured by signal strength and visually presented on a monitor. The signal strength is also converted to a corresponding audio tone by the signal processing units. The operator can then accurately locate the implanted tags by scanning the target area with the probe and reacting to changes in the tone; when the probe is placed closer to the tag, the system produces a higher pitch. The prototype system used in this animal experiment had an effective range of measurement of 7 mm, and the distance can be measured down to the millimeter level.

Animal Care

Animal care, housing, and surgery were performed with the approval of the Committee for Animal Research of Kyoto University, Japan, which ensures the humane treatment of laboratory animals in compliance with guidelines established by the Ministry of Education, Culture, Sports, Science and Technology, Japan. Seven dogs (age, < 2 years; body weight, 7.5-12.5 kg) were used in this study. Before the bronchoscopic procedures, all dogs were premedicated by intramuscular injection of 0.05 mg/kg atropine sulfate. They were then sedated with intramuscular injection of 15 mg/kg ketamine hydrochloride and 3 mg/kg xylazine hydrochloride. Local anesthesia of the upper respiratory tract was performed using a 1% lidocaine solution. For surgical procedures, dogs were intubated endotracheally under the same premedication and anesthetic sedation. Sevoflurane and nitrous gas were used for maintenance of anesthesia, under mechanical ventilation. Electrocardiogram and percutaneous oxygen saturation were monitored throughout the surgical procedures.

Preparation of SPLN-Imitating Pseudolesions and Selection of Target Lesions

Before the operation, pseudolesions imitating SPLNs were created by injecting 0.2 mL of colored collagen to lung peripheral parenchyma in a selected variety of lobes under CT guidance (Aquilion TSX-101A; Toshiba, Tokyo, Japan). The colored collagen solution was prepared as a mixture of 5 mL of 1% collagen solution and 5 mL of dye (5% indocyanine green or indigocarmine). A 23-gauge injection needle (NM-201L-0423; Olympus Corporation, Tokyo, Japan) was used for injecting the solution through the working channel of the bronchoscope (BF240; Olympus). A postprocedure CT scan was performed to confirm the size and location of each created lesion. Peripherally located pseudolesions with a diameter of approximately 10 mm were selected as target lesions for further experimentation.

Marking of the Target Lesions

The target lesions were marked within 2 days after creation for the subsequent operative procedures. Under a CT scan guide, an RFID tag was delivered into a small peripheral airway close to each target lesion. Through the 2-mm working channel of the bronchoscope, an introducer tube with a radiopaque marker on its distal tip was navigated to the target lesion (Figure 2). The tube was constructed from polytetrafluoroethylene (Teflon; DuPont Corporation, Wilmington, Del) and has an outer diameter of 1.8 mm. When the operator confirmed that the tip of the introducer tube was in the vicinity of the target lesion, the tag could then be implanted: the RFID tag was inserted from the proximal end of the tube and pushed out from the distal end by a flexible pusher-wire made of stainless steel. A postprocedure CT scan was performed to measure the distance from the tag to the nearest edge of the target lesion.

Operative Procedure

Immediately after tag delivery to the target lesions, the dogs were brought into an operating room and placed in a lateral decubitus position. With the animals under general anesthesia with intubation and ipsilateral lung collapse, the embedded tag and wedge resection of the target lesion were detected. Three ports with a 10-mm incision were set for each tag—1 for the scope and 2 for port access to the pleural cavity. Under thoracoscopic view, the lobe of interest was scanned with the locating probe to find the target lesion labeled with the tag. When the tag was localized, ring-shaped forceps were introduced from the other port to grasp the pleura just

ET/BS

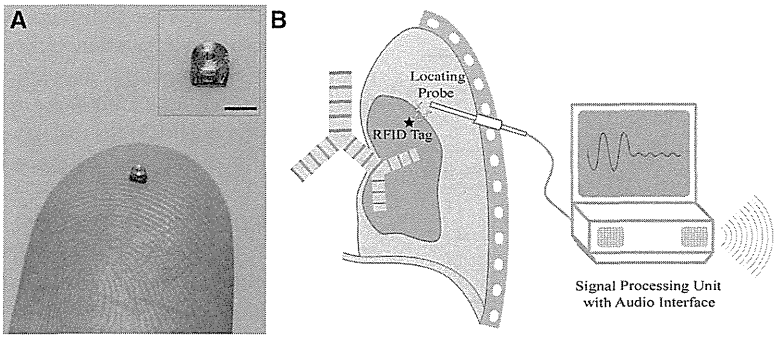

FIGURE 1. A, Photograph of a micro radiofrequency identification *(RFID)* tag on a forefinger (scale bar = 1 mm). The tag works as a passive transponder when it is activated by a radio wave of 13.56 MHz. B, Schematic diagram of the RFID marking system, including a wand-shaped locating probe for endoscopic use and a signal processing unit with an audio interface. The operator can locate the implanted tags by scanning the target area with the probe and responding to audio cues; when the probe is nearer the tag, the system produces a higher pitch.

above the site. After a reconfirmation of the tag position, the locating probe was pulled off and an endostapler was introduced from the same port to clamp the estimated resection line. Before the endostapler was fired, the locating probe was reinserted in place of the ring forceps to establish that the tag was contained within the lung tissue to be excised (Figure 3). Owing to the millimeter-level ranging capability of the system, an appropriate surgical margin could be ensured. When the lesion and the tag were resected with the endostaplers, the specimen was incised to measure the surgical margin.

Outcome Measures

The primary end point of this study was the rate of successful wedge resection of pseudolesions with good margins. Secondary measures were (1) the distance from the pseudolesion to the tag as shown in the confirmation CT, (2) the time required for the marking procedure, (3) the time required for tag detection at operation, and (4) the distance from the edge of the pseudolesion to the stapler line, which provides information on the surgical margins (Table 1). The median values and range were calculated for these measures. Finally, we analyzed the system's merits and pitfalls.

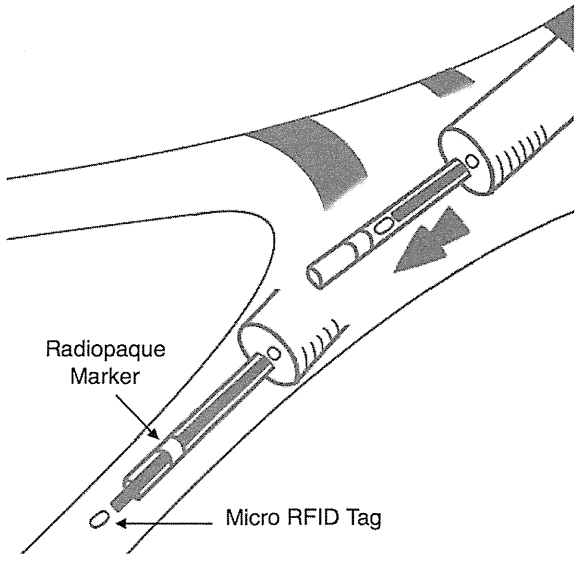

FIGURE 2. Illustration of the radiofrequency identification *(RFID)* tag delivery system. An introducer tube with a radiopaque marker on its distal tip is inserted through the 2-mm channel of a bronchoscope. The material of the tube is polytetrafluoroethylene (Teflon). An RFID tag is inserted from the proximal end of the tube and pushed out from the distal end by a pusher-wire.

RESULTS

A total of 14 pseudolesions were created by colored collagen injection in 7 dogs. Of the 14 pseudolesions, 10 had a diameter of approximately 10 mm and were selected as target lesions for further experimentation; there were 2 pseudolesions located in the right cranial lobes, 4 in the right caudal lobes, and 4 in the left caudal lobes. The other 4 pseudolesions were excluded because of larger diffusion or intrabronchial spread of injected collagen solution.

By means of the bronchoscopic marking procedures, each selected pseudolesion was accurately labeled with 1

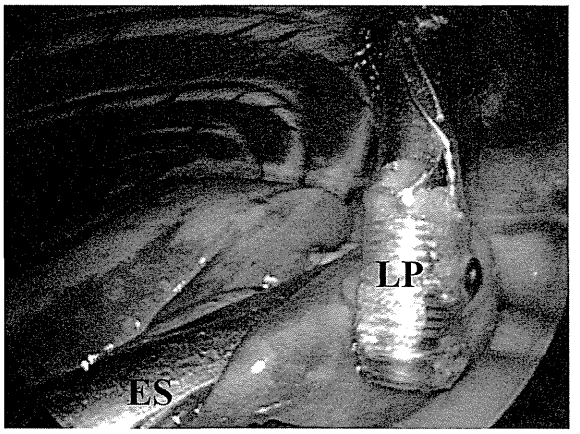

FIGURE 3. Thoracoscopic view of tag detection with a locating probe *(LP)* and resection of a pseudolesion in peripheral lung parenchyma. Before firing off the endostapler *(ES)*, the operator can confirm the position of the implanted tag to ensure an appropriate margin.

ET/BS

TABLE 1. Results of the primary end point and secondary outcome measures of the experiments

Primary end point		
Successful tag detection*	9/10	
Successful wedge resection*	9/10	
Secondary measures		**Median**
Time required for marking (min)	5-34	11
Distance from the lesion to the tag (mm)	0-6.5	2.1
Time required for tag detection (s)†	10-105	27
Surgical margin (mm)†	8-12	11

*One failure was due to dislocation of the tag. †n = 9.

RFID tag (Figure 4). The tags were placed at a median distance of 2.1 mm from the lesions (range, 0-6.5 mm, confirmed by postprocedure CT scan). The time required for the marking procedure ranged from 5 to 34 minutes (median, 11 minutes) from the insertion of the bronchoscope to the completion of the confirmation CT scan. Marking procedures were performed just after the creation and selection of the first 3 target pseudolesions and 1 or 2 days after creation for the other 7. No major complications such as pneumothorax or bleeding were observed.

During the thoracoscopic surgical procedures, 9 of the 10 implanted tags were successfully detected by the system. The time required for detection ranged from 10 to 105 seconds (median, 27 seconds). Subsequently, wedge resections were performed for these 9 lesions with a median margin of 11 mm (range, 8-12 mm). In the single nondetected case, a right upper lobectomy was performed only to find no tag in the resected lobe. The dislocated tag was later found in the endotracheal tube.

DISCUSSION

RFID is a wireless method of automatic identification originally developed for military radar systems in the 1940s to distinguish between friendly and enemy aircraft.[12] Currently, RFID tags are indispensable in modern society, with applications in item tracking for supply chain management, cashless payments for shopping, and personal identification for ticketing or entrance gates. The continuing miniaturization of RFID tags and development of computer networks have contributed to the widespread use of this system.

Applications have also developed in the field of health care: RFID technology has become widely used for personal identification of medical staff and for tracking drugs and medical equipment in so-called "smart hospitals."[13] Some reports have been published in which RFID technology was deployed to solve problems specific to medical practice. For example, Macario and colleagues[14] successfully detected surgical sponges labeled with RFID tags in the abdomen, Reicher and colleagues[15] reported the efficacious monitoring of the position of an RFID tag–labeled endotracheal tube at bedside, and Mayse and colleagues[16] experimentally implanted RFID tags in canine airways to achieve real-time tracking of tumor positions for stereotactic radiotherapy. In all these medical cases, RFID technology was used to detect the position of an embedded tag.

Our idea was to use micro RFID tags as wireless markers for locating SPLNs in thoracoscopic lung surgery. There is currently only a single previous report showing a similar concept in the field of breast surgery.[17] That study was essentially a proof of concept in a phantom study using large-sized tags (2 mm in diameter and 8 or 12 mm in length) responding to a radiofrequency of 134.2 kHz. To our knowledge, there has been no report on animal experiments or clinical trials of the system, although their tags (VeriChip; Verimed, Inc, Fort Lauderdale, Fla) have been approved by the United States Food and Drug Administration for human use. With the further advances in RFID technology, we have used 1-mm RFID tags in this study and confirmed their feasibility in an animal model for lung wedge resection.

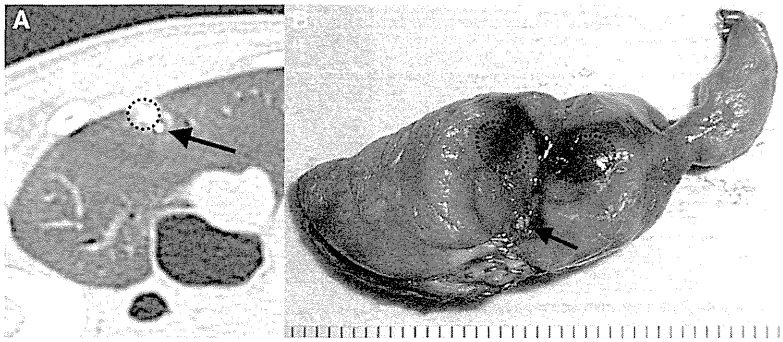

FIGURE 4. A, Computed tomography scan of a canine lung, including a pseudolesion created by colored collagen injection (areas surrounded by *black dotted line*) and an implanted micro radiofrequency identification tag *(black arrow)*. B, Photograph of a corresponding surgical specimen (scale bar = 1 mm).

ET/BS